

# **A novel method for the Holistic, Simulation Driven Ship Design Optimization under Uncertainty in the Big Data era**

**Lampros Nikolopoulos<sup>a</sup>, Evangelos Boulougouris<sup>b</sup>**

<sup>a</sup>School of Naval Architecture, Ocean and Marine Engineering, University of Strathclyde in Glasgow.

Email: lampros.nikolopoulos@strath.ac.uk

<sup>b</sup>Maritime Safety Research Center, School of Naval Architecture, Ocean and Marine Engineering,

University of Strathclyde in Glasgow. Email: evangelos.boulougouris@strath.ac.uk

## **Abstract**

The changing fuel costs, tough and volatile market conditions, the constant societal pressure for a «green» environmental footprint combined with ever demanding international safety regulations setup a completely new framework for commercial ship design. Ballast Water Treatment Systems, the ambitious IMO agenda for de-carbonization of shipping by 2050, the Goal Based Standards and most importantly the revision of the IMO MARPOL Annex VI, constitute a framework with strict and often contradicting requirements. On the other hand, the global economic uncertainty, rapid fleet growth and unsteady demand of commodities create a volatile economic operating environment for shipping companies.

Ship design needs to adapt to this new reality. Holistic approaches, with lifecycle considerations, aiming at robust designs are deemed necessary. Such a methodology is presented herein. It is built within the software CAESES and is consisted by a geometrical model core with several integrated modules that cover stability, strength, powering and propulsion, safety, economics, as well as an operation simulation module, enabling the user to

26 simulate the response in variations of the geometrical, design variables of the vessel under  
27 uncertainty. The latter is captured in several levels including Economic, Environmental,  
28 Operational uncertainty as well as the inaccuracy of the methods themselves.

29

30 Keywords: Holistic Ship Design Optimization under Uncertainty, Simulation Driven Design,  
31 Surrogate Models, Design for Efficiency, Big Data, Digital Twin.

32

### 33 1 INTRODUCTION

34 The first decade of the 21<sup>st</sup> century and the dominating economic recession combined with a  
35 fall in freight rates (due to tonnage overcapacity) has threatened the financial sustainability of  
36 numerous shipping companies. At the meantime, following the Kyoto protocol and the societal  
37 pressure for greener shipping gave birth to a number of international environmental regulations  
38 legislated by the UN International Maritime Organization (IMO) and classification societies  
39 that set the scheme for future as well as existing ship designs. Among others, future vessels'  
40 carbon emissions are controlled both by technical and operational measurements while ballast  
41 treatment facilities must also be incorporated in order to mitigate the risk of reduced  
42 biodiversity due to the involuntary carriage of evasive species inside water ballast tanks.

43 When focusing in the dry bulk cargo transportation, the carriage of major bulk commodities,  
44 i.e. iron ore, coal and grain the iron ore and coal dominate this market. According to the United  
45 Nations UNCTAD Report [2], in 2017 a record 1,364 million tons of iron ore and 1,142 million  
46 tons of coals have been transported by sea. The total dry bulk seaborne trade in 2017 totaled at  
47 4,827 million tons making iron ore and coal the dominant commodities with 28.3% and 23.7%  
48 of the total trade.

49 The bilateral trade for the two major commodities is in fact very specific. From one hand, the  
50 Chinese economy poses a constant demand for iron (for construction) and coal (for energy).

51 On the other hand the major iron ore exporters are located in South America (primarily Brazil)  
52 and Australia, while coal production in order of mil tons is concentrated in Indonesia, Australia  
53 and Russia with 383, 301, and 314 mil tons respectively. The present paper focuses on vessels  
54 intended for this trade which can be grouped in the Capesize / Very Large Ore Carrier (VLOC)  
55 segment of the shipping market. The design of such (and all) bulk carriers in general for the  
56 past decade (2008-2018) focused on the increase of efficiency by two means: increase of cargo  
57 carrying capacity and decrease of energy demands. In most cases the optimization, if any, is  
58 based on a single design point in terms of both speed and loading condition (draft and thus  
59 displacement) by the alternation of the local geometrical characteristics only. This paper in turn  
60 proposes the herein developed and proposed holistic methodology intended for the  
61 optimization of the basic design of large bulk carriers based on their actual simulated  
62 operational profile, for their entire lifecycle and under conditions of uncertainty. The speed and  
63 trading profile is simulated for the entire economic life of the vessel and the optimization  
64 focuses on the minimization of all operating costs, maximization of income, minimization of  
65 internal rate of return (IRR) summarized by the Required Freight Rate (RFR) from one hand  
66 and from the other the minimization of the energy footprint of the vessel expressed by the  
67 Energy Efficiency Design Index (EEDI) , simulated Energy Efficiency Operating Index  
68 (EEOI), lifecycle emissions as well as the minimization of the required water ballast amount  
69 for stability in order to minimize (or even eliminate) the energy and costs for the treatment of  
70 water ballast onboard.

71

## 72 2 OVERVIEW OF THE HOLISTIC METHODOLOGY

73 Holism, originating from the Greek word ὅλος (meaning all, entire, total), is the philosophical  
74 notion that all the properties of a given system (biological, chemical, social, economic, mental,  
75 linguistic, etc.) cannot be determined or explained by the sum of its component parts alone.

76 Instead, the system as a “whole” determines an important way how the parts behave. Aristotle  
77 in *Metaphysics* (H-6, 1045a8–10) (Aristotle, Ross [35]) examines the problem of the unity of  
78 definition and offers a new solution based on the concepts of potentiality and actuality.  
79 Although the concept of holism was pervasive, the term holism, as an academic terminology,  
80 was introduced by the South African statesman Jan Smuts in his 1926 book, *Holism and*  
81 *Evolution* (Smuts [50]) which defined holism as "The tendency in nature to form wholes that  
82 are greater than the sum of the parts through creative evolution".

### 83 2.1 Holistic Ship Design

84 The term Holistic Ship Design which is the core and basic notion and principle of the herein  
85 presented research work was first introduced by (Papanikolaou, [43]), where the generic ship  
86 design optimization problem is defined and presented in its holistic nature. The typical process  
87 flow of computational methodologies for performing all the necessary computations included  
88 in the different design aspects is also defined. Within the same context of Holistic Ship Design  
89 theory, the publication of (Papanikolaou, et al., [46]) , a product of a series of research projects,  
90 aimed at the systematic, Risk Based Optimization of AFRAMAX tankers (Papanikolaou, et al.,  
91 [45]), focusing on the cargo carrying capacity, steel weight and accidental oil outflow. The  
92 same design concept and computational methodology has been further refined and evolved in  
93 the publications of (Sames, et al. [48]), (Papanikolaou, et al [44]) as well as (Nikolopoulos [9]).  
94 Applications of holistic ship design optimization principles applied for container vessels by  
95 using a fully parametric hull surface modeled in CAESES ® coupled with NAPA for  
96 compartmentation can be found in the studies of (Priftis, et al., [47]) as well as the previous  
97 studies of (Soulтанias, [51]), (Koutroukis, et al., [41]) and (Nikolopoulos, et al., [42]). Subject  
98 model was originally developed for the parametric design and optimization of a novel  
99 containership with ellipsoidal mid-ship section in (Koutroukis, [13]) and is based on the same

100 principle of parametric design and optimization as the tanker optimization studies previously  
101 presented.

102 Using the above work and their previous work and development of such design methodologies  
103 within the Ship Design Laboratory of the National Technical University of Athens, Authors  
104 herein present an evolved and further enhanced method fully incorporated in the CAESES ®  
105 CAD/CAE environment.

106 The methodology is holistic, in the sense that all of the critical aspects of the design are  
107 addressed under a common framework that takes into account the lifecycle performance of the  
108 ship in terms of safety efficiency and economic performance, the internal system interactions  
109 as well as the parameter correlations, design trade-offs and sensitivities. The workflow of the  
110 methodology has the same tasks as the traditional design spiral with the difference that the  
111 approach is not sequential but concurrent.

## 112 2.2 Simulation Driven Design

113 The embedding of a vessel's operation simulation within the early design process has not been  
114 adequately studied in the literature with only a handful of relevant examples available. Within  
115 the direction of simulation in early ship design, (Tillig, et al. [52]) propose a generic ship energy  
116 systems model that can predict the ship's energy consumption during different operational  
117 conditions, without however taking into account variation of the vessel's RPM, heavy running  
118 and potential limitations from the engine's torque (fuel) limit. In (Alwan et al [34]), an event-  
119 based simulation model is utilized in order to reduce the simulation cost using an event based  
120 operational profile instead of time-domain simulation of vessel operation, using discrete event  
121 simulation for analyzing system performance. A quasi-static discrete-event simulation model  
122 to replicate and assess the voyage of a general cargo vessel is proposed by (Sandvik, et al. [49])  
123 using a prescribed route based on real time (15 minute) data and a constant speed assumption  
124 and could be potentially integrated in a design environment.

125 The primary novelty of the herein presented methodology is that it is simulation driven in the  
126 sense that the assessment of the key design attributes for each variant is derived after the  
127 simulation of the vessel's operation under different voyage profiles for its entire lifecycle  
128 instead of using a prescribed loading condition and operating speed (Nikolopoulos,  
129 Boulougouris [17]). The operation simulation takes into account the two predominant trade  
130 routes large bulk carriers are employed in using actual, real-time operating data from a fleet of  
131 large bulk carriers (Capesize and Newcastlemax). By employing such a technique, the actual  
132 operating conditions and environment with all uncertainties and volatilities connected to the  
133 latter is used to assess the merits of each variant of the optimization ensuring that the design  
134 will remain robust and attain its good performance over a range of different environments and  
135 for its entire lifecycle. The dimensioning of the principal components, e.g. the main engine and  
136 propeller is based on the margin allowed from a limit state condition assumed in the analysis.

### 137 2.3 Design under Uncertainty

138 The effects of uncertainty during all stages of Ship Design as well as its implications in  
139 Optimization studies is a well-studied topic in the literature with notable examples the works  
140 of (Hannapel, [39]) , (Hannapel & Vlahopoulos, [40]), examining two methods of Uncertainty  
141 modeling for ship design optimization, that of robust optimization and reliability-based  
142 optimization. An example of reliability-based design use of uncertainties in a Ship Design  
143 Multi-Disciplinary Optimization model is that of (Good, [38]). A two-stage stochastic  
144 programming for robust ship design optimization under uncertainty has been developed by  
145 (Diez & Peri, [36]), (Diez, et al., [37]).

146 For the present work, a comprehensive approach with regards to the uncertainty and the  
147 statistical modelling of the latter is followed as at the following distinctive levels/elements:

148 a. Weather and Environmental Uncertainties

149 b. Shipping Market Uncertainties

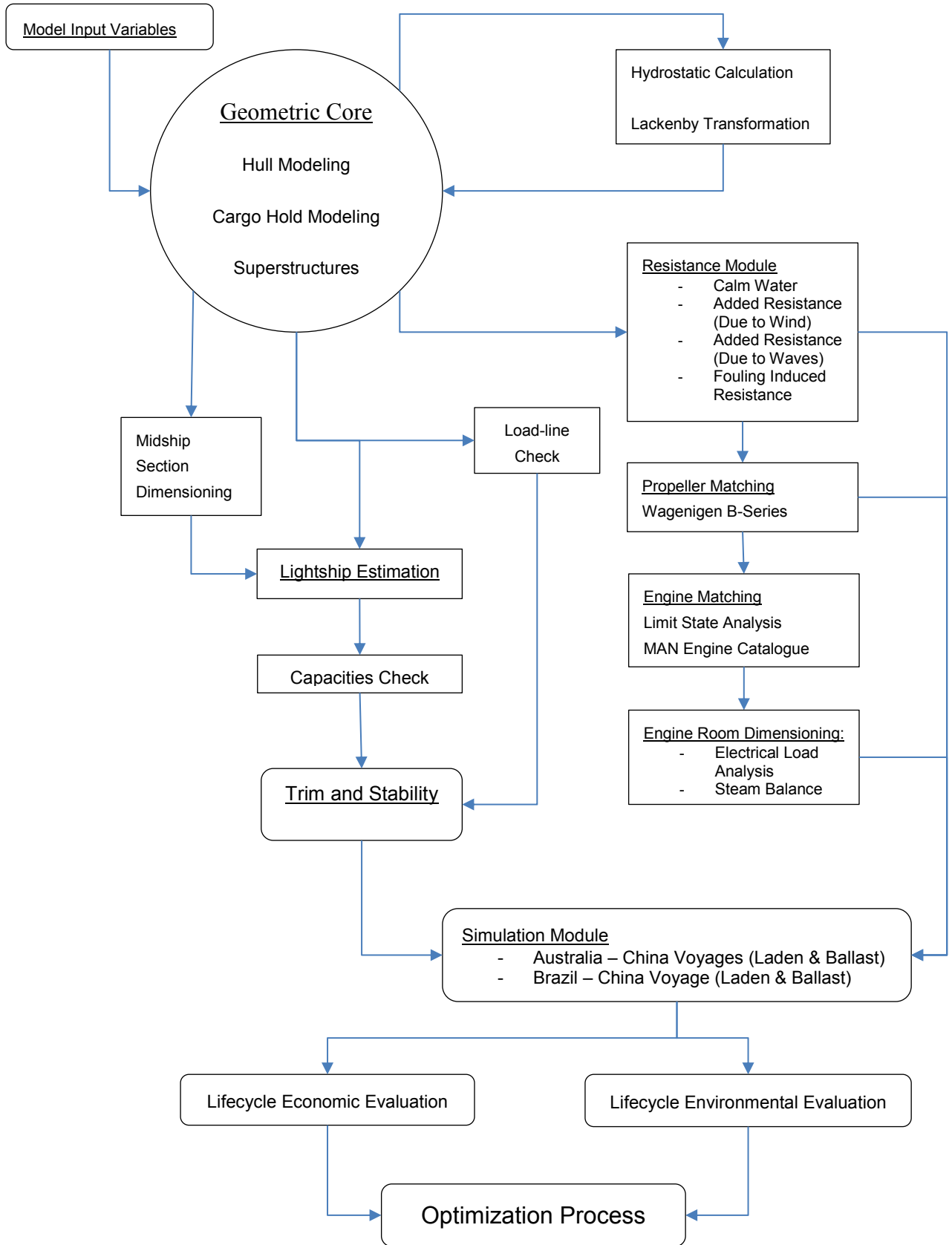
### 150 c. Methodology Uncertainty and Error Modeling

151 Missing values are a common issue in large data analysis. Missing data leads both to bias as  
152 well as loss of information. There are various ways of treating them. There is the “complete  
153 case” (Nguyen, Carlin, and Lee 2017) approach which discards individual observations  
154 containing missing data to provide only a dataset with completed observed data. Another  
155 method used is the data imputation (Little and Rubin 2019). Imputation is fundamentally a  
156 further layer of modelling whereby missing values are estimated from other predictor variables  
157 in the dataset. We have applied both as a systematic filtering of real-time data, and as generation  
158 of Probability Distribution Functions for the Speed, Wind, Waves and other voyage parameters  
159 that in turn are used as input in the simulation module.

### 160 2.4 Design and Simulation Environment

161 The environment in which the methodology is programmed and is responsible for the  
162 generation of the fully parametric hull surfaces is the CAESES CAE which is a CAD-CFD  
163 integration platform developed for the simulation driven design of functional surfaces like ship  
164 hulls, propeller and appendages, but also for other applications like turbine blades and pump  
165 casings. It supplies a wide range of functionalities or simulation driven design like parametric  
166 modeling, integration of simulation codes, algorithms for systematic variation and formal  
167 optimization. The holistic methodology proposed has the workflow depicted in Figure [1].

START



END

169 Figure 1: Workflow of the Proposed Methodology

## 170 2.5 Geometric Core

171 The core of this methodology and any similar developed in a CAD/CAE system is the  
172 geometrical model (geometrical core). The original surface is produced as group of parametric  
173 sub-surfaces modeled in the CAESES.

## 174 2.6 Initial Hydrostatic Properties

175 The hydrostatic calculation aims on checking the displacement volume, block coefficient and  
176 center of buoyancy of the design. It is performed by an internal computation of CAESES and  
177 for its execution a dense set of offsets (sections) is required as well as a plane and a mirror  
178 plane.

## 179 2.7 Lackenby Variation

180 In order to be able to control the desired geometrical properties of the lines, and more  
181 specifically the block coefficient ( $C_b$ ) and the longitudinal centre of buoyancy (LCB), the  
182 Lackenby variation [32] is applied. This variation is a shift transformation that is able to shift  
183 sections aft and fore accordingly. Instead of applying quadratic polynomials as shift functions,  
184 fairness optimized B-Splines are used allowing the selection of the region of influence and the  
185 smooth transition as well. The required input for the transformation is the extent of the  
186 transformation which in this case is from the propeller position to the fore peak and the  
187 difference of the existing and desired  $C_b$  and LCB as well<sup>9</sup>.



188

189 Picture 1: Hull form surfaces following Lackenby variation with corresponding SAC curves

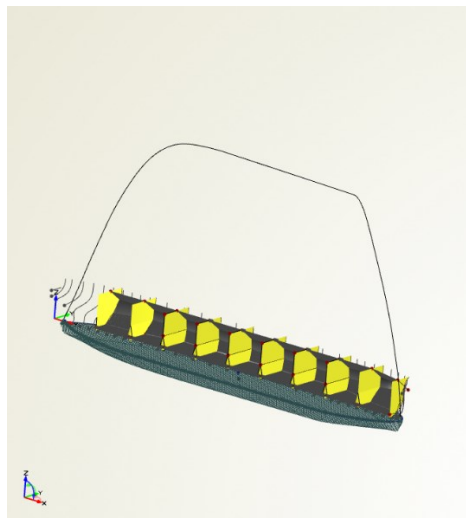
## 190 2.8 Cargo Hold Modeling

191 Using the output surface from the Lackenby variation, the cargo hold arrangement is generated  
192 with a feature of the CAESES and its capacity is calculated.

193 The cargo hold surfaces and their respective parametric entity were realized within CAESES.  
194 Furthermore, the hydrostatic calculations of CAESES were used to calculate the capacity of  
195 the cargo holds, which is necessary for most of the computations. The parameters/variables  
196 that are used for the Cargo Hold arrangement generation are the positions of the bulkheads, the  
197 position of the Engine Room bulkhead, the frame spacing as well as some local variables such  
198 as the hopper width and angle, the topside tank dimensions (width and height), the lower stool  
199 height and length and double bottom height.

200 The capacity of each tank is calculated by creating offsets for each one of the tank surfaces and  
201 joining them together. Afterwards, a hydrostatic calculation of the tanks takes place and the  
202 total capacity can be estimated and cargo density checked. Furthermore, a calibration factor  
203 derived from the parent hull is introduced in order to take into account the volume of the  
204 structural frames inside the cargo holds as well as a factor in order to derive with the Bale and  
205 Grain capacities.

206 The result of the parametric tank modeling can be also seen at the CAESES snapshot (picture  
207 [2])



208

209 Picture 2: Parametric Cargo Hold surfaces

## 210 2.9 Resistance Prediction

### 211 2.9.1 Calm Water Resistance

212 The resistance prediction of this model uses a hybrid method and two different approaches,  
213 depending on the optimization stage.

214 Initially, during the design of experiment and the global optimization phase, where a great  
215 number of variants is created there is a need for high processing speed and subsequently  
216 computational power. For this particular reason the Approximate Powering Method of Holtrop  
217 [6] is used that derives from experimental data and is a very fast method. Especially in bulk  
218 carriers it is very accurate too, since the wave making resistance as well as the viscous pressure  
219 resistance are very small fractions of the total resistance with the frictional resistance (direct  
220 function of the wetted surface) dominating all resistance components due to the dimensions  
221 and very small Froude number. The only inaccuracy of this method can be identified in the  
222 local viscous resistance effects and is common to all prediction methods.

223 However, in order to improve the prediction accuracy, especially for of design conditions such  
224 as the ballast condition, the coefficients for each component of the resistance used in Holtrop

225 and Mennen methodology were recalibrated against the parent vessel model tests while the  
226 coefficients used for the powering prediction were calibrated both from model tests and  
227 analytical CFD calculations on the parent vessel (Nikolopoulos and Boulougouris [18]). In  
228 subject publication the constants and parameters from Holtrop and Mennen approximate power  
229 method were systematically varied with use of genetic algorithms with the goal of calibrating  
230 the method for minimum error against the statistical database used. The calibration database is  
231 consisted by the model tests (in both design, scantling and ballast loading conditions) of 7  
232 different vessels with very similar geometric characteristics (full hull forms) and Froude  
233 number of the parent and target vessels. In total 111 points of power vs. speed for the Laden  
234 conditions and 61 points of power vs. speed for the Ballast conditions were assessed.

235 The calibration was performed by a systematic optimization approach. The optimization  
236 variables were the statistic coefficients as well as power values used in Holtrop methodology  
237 with a relatively big margin of variance as well as the introduction of some additional terms in  
238 existing equations. Then the methodology would be applied for each speed /power point of the  
239 model tests and the difference in powering would derive. The minimization of this difference  
240 is the optimization target of this particular sub problem. The applied algorithm for the  
241 optimization was the NSGA II [Deb, 33] with roughly 4,000 variants being produced in two  
242 steps for each condition. The first step was the calibration of the equations for the calculation  
243 of the bare hull resistance and power (EHP-Effective Horse Power) while the second calibrated  
244 the equations for applying the self-propulsion problem and thus calculating the delivered horse  
245 power (DHP). The result was an average difference of -4.3% and -0.20% of the EHP and DHP  
246 respectively, for the Ballast Condition and -1.94% and -6.5% of the EHP and DHP respectively  
247 for the Laden Conditions with the Holtrop results being more conservative (over estimation)  
248 than the model tests. The standard deviation, variances as well as a full statistical analysis was  
249 produced and the prediction error of the methodology was modelled in the IBM SPSS with a

250 non-linear regression method as a function of the vessels dimensions, block coefficient and  
 251 wetted surface and subsequently programed in the methodology.  
 252 The entire Holtrop method is programmed within the Framework and is also generated as a  
 253 feature for later use. Actual data from the geometric model is also used, such as the entrance  
 254 angle, prismatic coefficients etc., making the process more precise and representing of the  
 255 specific design.

### 256 2.9.2 Added Resistance due to Wind

257 The vessel's added resistance due to wind is calculated for two separate occasions in subject  
 258 methodology. The first being for the assessment for sizing the main engine at a prescribed  
 259 condition for the latter and second, within the simulation of the vessel's operation for each leg  
 260 and stage of the simulated voyage route. The tool used for the resistance is the formula of  
 261 Fujiwara et al [24] which is also used in the ISO15016-2015 [20] when doing corrections in  
 262 the measurements obtained in sea trials. Subject method is considered as reliable, robust and  
 263 accurate as the formula contains sensitivities and correlations with the hull and deckhouses  
 264 geometry (via the use of projected surfaces).

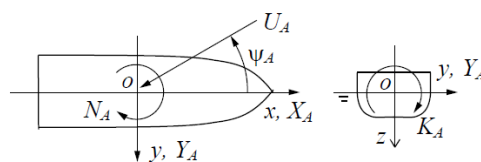
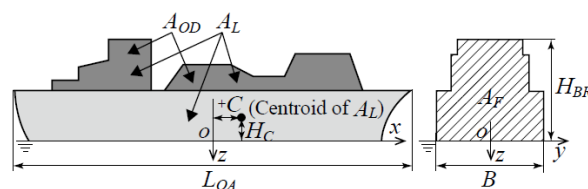


Fig. 1 Coordinate system.



265  
 266 Figure 2: Coordinate system and input used in Fujiwara empirical formula for the estimation  
 267 of added resistance due to wind [24].

### 268 2.9.3 Added Resistance due to Waves

269 The added resistance due to waves is similarly used in the two modules mentioned previously,  
270 namely main engine sizing and operational simulation. The tool used for the added resistance  
271 estimation is different depending on the stage of the optimization. For the initial stage,  
272 empirical formulae based on the Maruo far field are utilized while in a second stage, integrated  
273 panel codes using potential theory to solve the seakeeping motions problem and then through  
274 added mass calculate the added resistance. For the first stage, after assessing the method of  
275 Kwon et al [14, 15] as well as STAWAVE2 (as presented in ISO15016-2015 [20]) the new  
276 method of Liu et al. [25] for the estimation of added resistance in head waves is chosen instead.  
277 The method of Liu and Papanikolaou offers a fast and efficient calculation alternative to  
278 running a panel code, strip theory code or using RANS codes. The formula is based on best  
279 fitting of available experimental data for different types of hull forms. The formula, has been  
280 simplified to the extent of using only the main ship particulars and fundamental wave  
281 characteristics for the estimation of ship's added resistance.

282 The formula takes the below form:

$$283 \quad R_{AW} = R_{AWR} + R_{AWM} \quad (1)$$

$$284 \quad R_{AWR} = \frac{2.25}{2} \rho g B \zeta_a^2 a_d \sin^2 E \left( 1 + 5 \sqrt{\frac{L_{pp}}{\lambda} Fn} \right) \left( \frac{0.87}{C_B} \right)^{1+4\sqrt{Fn}} \quad (2)$$

$$285 \quad R_{AWM} = 4 \rho g \zeta_a^2 B^2 / L_{pp} \bar{\omega}^{b_1} \exp \left[ \frac{b_1}{d_1} (1 - \bar{\omega}^{d_1}) \right] a_1 a_2 \quad (3)$$

### 286 2.9.4 Fouling Related Resistance

287 The last environmental related added resistance factor taken herein into account both in the  
288 design modules (propulsion prediction and main engine selection) as well as input in the  
289 operational simulation module is that of marine biological fouling. More specifically, as the  
290 hull of the ship ages the average roughness value increases due to hull biological fouling. The

291 effect of the hull roughness for the vessel's resistance can be calculated from the below formula  
292 (International [21]):

$$293 \frac{\Delta R}{R} = \frac{\Delta C_F}{C_T} = 0.044 * [(k_2/L)^{1/3} - (k_1/L)^{1/3}] \quad (4)$$

294 With  $k_2$  and  $k_1$  being the current and previous hull roughness respectively. The hull roughness  
295 increase on an annual basis is also estimated from [International [22]] which starts from an  
296 average and continues on an exponential rate. Furthermore, in order to further enhance the  
297 lifecycle considerations, the dry docking recoating is taken into account in the 5, 10, 15, 20 and  
298 25 year interval with a reduction of the roughness to a level 10% higher than the previous  
299 coating system (e.g. roughness in 5 years is 10% higher than the newbuilding value, roughness  
300 in 10 years is 10% than the 5 year value etc.). The starting roughness value at the delivery stage  
301 of the vessel is assumed to be an average value of 97.5 microns (average of minimum reading  
302 of 75 $\mu$  and maximum reading of 120 $\mu$ ).

303 The power increase corresponding to the above resistance increase is approximated by the  
304 following formula (International [19]):

$$305 1 + \frac{\Delta P}{P} = \frac{1 + \Delta R/R}{1 + \Delta \eta/\eta} \quad (5)$$

306 With the increase on the propeller open water efficiency being:

$$307 \frac{1}{1 + \Delta \eta/\eta} = 0.30 * \left(1 + \frac{\Delta R}{R}\right) + 0.70 \quad (6)$$

308

## 309 2.10 Propeller Model

310 While the vessel's Propeller is not modelled geometrically at this current stage, it is assumed  
311 to be a part of the Wageningen B-Series of propellers. All the Wageningen polynomials are  
312 modeled within the methodology (Bernitsas [19]) so the open water diagrams of a propeller  
313 with a selected pitch, diameters, blade number and expanded area ratio can be derived.  
314 Following this, the self-propulsion equilibrium is conducted in the design speed in an iterative

315 manner in order to derive the final propulsion coefficients, shaft horse power, torque, thrust  
316 and propeller revolutions (RPM). This is in turn used for the propeller-engine matching and  
317 the propulsion plant dimensioning.

318 The optimal selection of the propeller parameters (diameter, pitch, blades) is also part of the  
319 global/preliminary design stage

320

## 321 2.11 Main Engine and Engine Room dimensioning

### 322 2.11.1 Main Engine

323 After the propeller is dimensioned, the Main engine should be matched to that hull and  
324 propeller. In order to avoid the well-known (and rather recent) risk of underpowered vessels,  
325 instead of employing a weather and fouling margin (typically 15%), a dimensioning condition  
326 was in turn used as determined by users. This condition is such that the vessel should maintain  
327 the full speed and corresponding engine load, power and RPM at head and beam waves  
328 corresponding to sea state 5, with adverse (head) current of 1.5 knots, roughness due to fouling  
329 corresponding to 4 years without cleaning and the corresponding head wind of sea state 5. In  
330 addition to the power requirements of the above an RPM of 10% (in accordance with MAN  
331 B&W requirements [7]) is imposed as well as an additional margin of 5% which is considered  
332 for derating the main engine and ensuring smaller Specific Fuel Oil Consumption (SFOC).

333 For the final requirements the main engine is matched with the existing “G-Type”, “ultra-long stroke”,  
334 engines available from MAN [7]. Firstly an “engine library” with alternative configurations is  
335 created, which is utilized in the selection module in combination with an internal iterative  
336 procedure ensures that the engine will have sufficient light running margin and that the layout  
337 point on the diagram is close to the L2L4 line corresponding to bigger torque/MEP margins  
338 and smaller SFOC values. A Final SFOC curve from 10% to 100% is produced and corrected  
339 for the actual engine layout.

340 All engines within the engine selection library are Tier III compliant in accordance with the  
341 MARPOL Annex VI, Regulation 13 as amended by the IMO MEPC 66 requirement [26] for  
342 ships built after the 1<sup>st</sup> of January of 2016.

343 In addition to SFOC curves, curves of steam production from 20% to 100% are produced.  
344 These are used in turn as steam production curves in the operation simulation, in order to assess  
345 the potential load (if required) of the composite boiler to match the steam consumption  
346 requirements.

### 347 2.11.2 Diesel Generators

348 The electrical balance analysis of the parent vessel is normalized with the derived SMCR for  
349 each consumer and each condition respectively and the ratios are used within the methodology  
350 to determine the load of each consumer for the generated variants and thus the electrical load  
351 for each condition. The required alternator output is calculated based on this (after including a  
352 safety factor), while the prime movers (diesel generators) of the alternators are sized by  
353 assuming an 85% electrical efficiency.

### 354 2.11.3 Exhaust Gas Boilers

355 Similarly to the case of the electrical balance, the steam balance of the vessel is also non-  
356 dimensionalized. For applications of fuel tank heating (whether bunker or settling/service  
357 tanks) the steam consumption (in kg/h) is non-dimensionalized by the fuel tank capacity  
358 (calculated in intact stability module).

## 359 2.12 Lightship Weight Prediction

360 The lightship calculation follows the traditional categorization in three weight groups, the  
361 machinery weight, the outfitting weight and the steel weight.

### 362 2.12.1 Machinery Weight

363 The machinery weight calculation is based on the average of two methods: the Watson-Gilfillan  
364 formula and the calculation based on the Main Engines weight respectively.

365 The machinery weight estimation is based on a empirical formula due to Watson-Gilfillan<sup>5</sup>:

$$366 \quad Wm = Cmd * Pb^{0.89} \quad (7)$$

367 The average is used to balance out any extreme differences, and the coefficients of the Watson-  
368 Gilfillan formula are calibrated for low speed, two stroke engines based on statistic data  
369 available for a fleet of bulkers.

### 370 2.12.2 Outfitting Weight

371 The outfitting weight is also based on the average of two independent calculations. The  
372 Schneekluth method is one and the use of empirical coefficients for sub-groups of that  
373 particular weight group is the other one.

### 374 2.12.3 Steel Weight

375 During the initial design stages, and the selection of optimal main dimensions, it is necessary  
376 to identify the effect of the change of the principal dimensions of a reference ship on the  
377 structural steel weight. Thus, at first, an accurate calculation of the steel weight of the reference  
378 ship is conducted. Following this, the "Schneekluth Lightship Weight Method" was applied  
379 [Papanikolaou, 7]. Given that the steel weight for the parent vessel was available as derived  
380 from summing the individual steel block weights (from the shipbuilding process) a TSearch  
381 algorithm was employed in order to vary the values of the statistical coefficients and constants  
382 of subject methodology with the objective of the minimization of the difference between the  
383 actual and calculated values for the steel weight. The result was an accuracy of 0.3% which is  
384 more than acceptable within the scope of basic/preliminary design. The error was modeled  
385 also in the IBM SPSS as a function of the principal particulars and block coefficient.

### 386 2.13 Deadweight Analysis

387 The deadweight of the vessel is composed of subgroups such as the consumables, the crew  
388 weight and the deadweight constant. The Deadweight analysis is the prediction of the payload  
389 of the vessel based on the calculation of the consumables.

390 As mentioned before, the consumables for the machinery is calculated, namely the Heavy Fuel  
391 Oil for the main engines, and diesel generators, the Lubricating Oils of the engines and  
392 generators.

393 Furthermore, based on the number of the crew members (30), the fresh water onboard is  
394 calculated as well as the supplies and the stores of the vessel.

#### 395 2.14 Stability and Load-line Check

396 The initial intact stability is assessed by means of the metacentric height of the vessel (GM).  
397 The center of gravity of the cargo is determined from the capacity calculation within the  
398 framework while the center of gravity for the lightship and consumables is determined from  
399 non-dimensioned coefficients (functions of the deck height) that derive from the information  
400 found in the trim and stability booklet of the parent vessel. All the above are calculated with  
401 the requirements of the IMO Intact Stability Code for 2008 [IMO, 5].

#### 402 2.15 Operational Profile Simulation

403 This module is an integrated code within the methodology that simulates the actual operating  
404 conditions of the vessel for its entire lifecycle. Two trade routes are considered, the Brazil to  
405 China roundtrip and the Australia to China roundtrip. Each voyage is split into legs depending  
406 on distinctive sea areas.

407 For the Australia to China roundtrip the following legs are considered:

- 408 • Leg A: Sea Passage from W. Australia loading ports to Philippines being subdivided into 4  
409 sub-legs.
- 410 • Leg B: Sea Passage from Philippines to Discharging port being subdivided into 4 sub-legs.
- 411 • Leg C: Only for the ballast leg to Australia a stop in Singapore for bunkering is considered.

412 For the Brazil to China roundtrip the following legs are considered:

- 413 • Leg A: Sea Passage from the Brazilian Loading port to the Cape of Good Hope in South  
414 Africa. This leg is subdivided into 4 equal sub-legs.

- 415 • Leg B: From the Cape of Good Hope in S. Africa to Indonesia and is subdivided into 4 equal  
416 sub-legs.
- 417 • Leg C: Sea Passage through the Malacca straight and Singapore including a port stay in  
418 Singapore for bunkering operations.
- 419 • Leg D: Sea Passage from Singapore through the Taiwanese straight into the discharging port  
420 of China. This leg is subdivided into to 2 sub-legs.

#### 421 2.15.1 Input Data

422 For each one of the legs (given distance in nautical miles) the average speed and added  
423 resistance curves are input as well as the loading of the generators, the maneuvering time. If  
424 the leg includes a discharging, loading or bunkering port the port stay in hours is also used.  
425 Based on this profile the voyage associated costs together with the fuel costs are calculated on  
426 a much more accurate and realistic basis.

427 The input variables of the operation simulation model for each model can be seen in the below  
428 table [1].

429

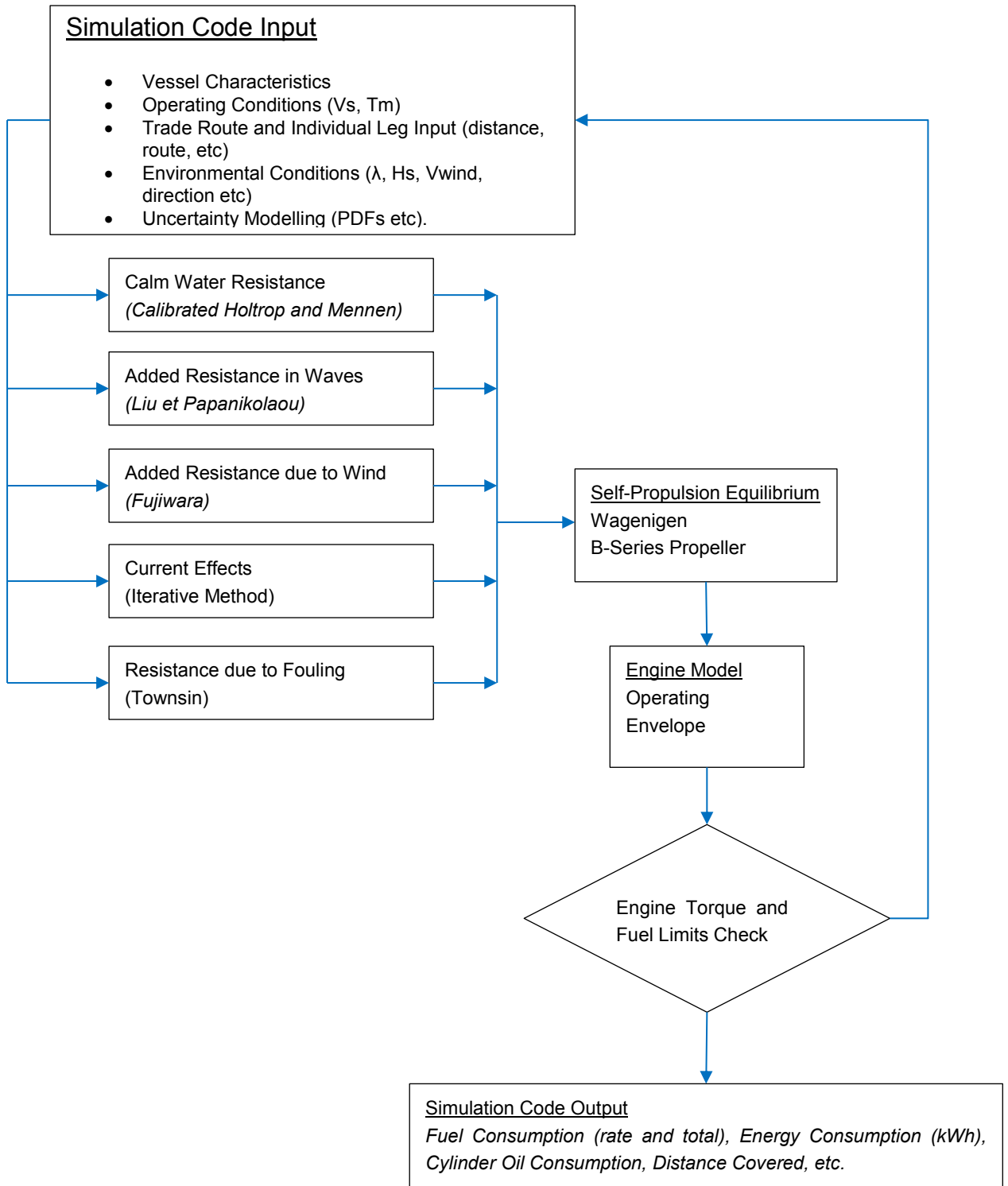
<b>Operational Simulation Input Parameters</b>	
<b>General</b>	
ISO corrected SFOC Curve	Speed Power Curve - Calm Water
Auxiliary Engines Power (kW)	SFOC curve for auxiliary Engines
Auxiliary Engine Load during Cargo Hold Cleaning (%)	Time for Cargo Hold Cleaning (hours)
Main Engine SMCR (kW)	Main Engine Load in Manoeuvring (%)
Cylinder Oil Feed Rate (normalized average) (gr/kWh)	Electrical Power Required during Normal Sea Going (kW)
Blowers Electrical Power (kW)	Required Electrical Power during Manoeuvring (kW)
Main Engine SFOC during Manoeuvring (gr/kWh)	Sulphur Content in Fuel (%)
<b>Main Dimensions</b>	
Length Overall (m)	Length Between Perpendiculars (m)
Breadth (m)	Voyage Draft (m)
Wind Profile	
Total Lateral Projected Area (m <sup>2</sup> )	Total Transverse Projected Area (m <sup>2</sup> )
Lateral Projected Area of Superstructures above deck (m <sup>2</sup> )	Fujiwara Hc (m)
Height of Superstructures (m)	
<b>Added Resistance</b>	
Wave Length Probability Distribution Function Curve	Entrance Angle Length (m)
Roughness Increase due to fouling (microns/year)	
<b>Propulsion</b>	
Thrust Deduction Curve	Wake Fraction Curve
Propeller Diameter (m)	Expanded Area Ratio (m <sup>2</sup> )
Number of Blades	Pitch over Diameter Ratio
Propeller Shaft Mechanical Efficiency	Relative Rotative Efficiency
Speed – RPM Curve	
Electrical Loads during Loading (kW)	Time in Loading/Discharging Port (hours)
Time for maneuvering (hours)	
<b>Sea Passage Leg</b>	
Distance (nautical miles)	Average Transit Speed (knots)
Probability of Head Current	Probability of Astern Current
Low Current Velocity (knots)	Mid Current Velocity (knots)
High Current Velocity (knots)	
<b>Sea Passage Leg – Singapore (additional)</b>	
Manoeuvring Time (hours)	Electrical Load in Port (kW)
Port Stay for Bunkering (hours)	

430

Table 1: Operational Simulation Input Parameters

431

The process flow of the simulation code is also depicted in figure [3].



432

433

Figure [3]: Process flow of the vessel operation simulation code.

#### 434 2.15.2 Added Resistance

435 For each leg, stage and corresponding time step the added resistance module is called from  
436 within the operational simulation module in order to calculate the added resistance. The final  
437 estimation is a probabilistic one, which means that the added resistance for different wave  
438 directions, wave heights and wave lengths is estimated and then a probabilistic figure is derived  
439 based on the probability distribution functions modeled from the onboard measurement data.

#### 440 2.15.3 Environmental Parameters Modeling

441 The operating speed for which the added resistance (and thus added propulsion power) is  
442 calculated is also probabilistic.

443 Initially the uncertainty of the average operating speed per leg is applied. The probabilities of  
444 having a  $\pm 15\%$  deviation from the estimated average of each leg are calculated from the  
445 probability density function derived from onboard data analysis. A probabilistic steaming  
446 speed is then produced from the weighted average of the higher and lower speeds.

#### 447 2.15.4 Currents

448 The second source of uncertainty with regards to the operating speed is environmental and is  
449 related to the local currents. For each leg/sea area a statistical analysis from onboard collected  
450 data, reveals both the average as probability distribution of the current speed and current  
451 direction. In the simulation module these calculated probability distribution functions are used  
452 in order to estimate the probability of encountering a high, medium and low current (their  
453 amplitude is determined from the minimum, maximum and average speed from the onboard  
454 data). The correction to the operating speed is positive for the cases of astern current and  
455 negative for ahead current. The ahead and astern currents are considered for an “operating  
456 envelope” of  $\pm 45$  degrees both in the ahead and astern term, as the side currents will only yield  
457 deviation rather than speed loss.

458 From the above mentioned two corrections the probabilistic ship speed is derived based on  
459 which both the calm water required delivered power is calculated as well as the added  
460 resistance and power calculations takes place.

#### 461 2.15.5 Fouling

462 The fouling margin, is also calculated depending on the age of the vessel in the respective  
463 simulation stage by calling the fouling resistance calculation module described previously.

#### 464 2.16 Economic Model

465 In total the code calculates the Operational Expenditure (OPEX), the Capital Expenditure  
466 (CAPEX), the Required Freight Rate (RFR), the Internal Rate of Return (IRR) as well as the  
467 IMO Energy Efficiency Operational Index (EEOI).

468 The Economic model also follows the principle of simulation driven design and design under  
469 uncertainty. The uncertainties in the economic model can be identified both in terms of the  
470 shipping market as well as the fuel prices which directly affect the fuel costs (burden to owners  
471 that operate in the tramp/spot markets).

472 The market uncertainty is predominately expressed by the uncertainty of the vessel's Earnings.  
473 Through the Clarkson's Shipping intelligence database (Clarkson's [23]), a probability  
474 distribution function for the Capesize earnings was produced based on the data from 1990 to  
475 2015 which cover a typical vessel's economic (and engineering) lifetime. Based on the earnings  
476 the probability of high (150,000 USD/day TCE), mid (35,000 USD/day TCE) and low (5,000  
477 USD/day TCE) were calculated and thus a probabilistic value for the vessel's annual as well  
478 as lifecycle (by applying the interest rates) profitability was derived. Apart from this earnings  
479 directly affect the other shipping markets, namely the acquisition market (both the S&P and  
480 Newbuilding market; for the case herein presented the second as well as the scrap market. For  
481 this particular reason and in order to further enhance the correlation to the vessel's design the  
482 newbuilding prices and scrap prices were expressed (after suitable adjustment) per ton of

483 lightship and were correlated from the Clarkson's Shipping Intelligence database to the  
484 Earnings of the vessel with the following formulas:

$$485 \text{ NBprice} = 157.335 * \text{Earnings}^{0.269} \quad (8)$$

$$486 \text{ Scrap\_price} = 25.648 * \text{Earnings}^{0.244} \quad (9)$$

487 For both equations the value returned is USD/ton of lightship and serve as magnification factors  
488 for the acquisition and residual values of the vessel. Furthermore, the two last which are used  
489 for the CAPEX calculation, are also probabilistic by applying the same probabilities that are  
490 used for High, Mid and Low Earnings with the respective amounts introduced in the above  
491 presented formulas. By this way, it is able to accurately depict the volatility of the market and  
492 the response of each design variant as well as the effect of its dimensions to its lifecycle  
493 economic performance.

494 This is further enhanced by the calculation of the Fuel Price cost which is outside the usual  
495 time charter provisions of bulker Charter Party agreements. The Fuel prices cost is also  
496 probabilistic with the probabilities for High (1500 USD/ton), Mid (450 USD/ton) and Low  
497 (150 USD/ton) prices being derived from the probability distribution function that was  
498 calculated from the Clarkson's Shipping Intelligence Database.

499 This is a key point of this methodology, namely to optimize the vessel's design under  
500 uncertainty as the produced designs correspond to a more realistic scenario and the dominant  
501 variants of the optimization have a more robust behavior over a variety of exogenous governing  
502 market factors.

503 The derived probabilistic values of RFR and the deterministic value of the EEOI are the  
504 functions/targets used in the optimization sequence later.

505

## 506 2.17 Energy Efficiency Design Index Calculation

507 The Energy Efficiency Design Index (EEDI) is calculated according to the formula proposed  
508 in the IMO resolution MEPC.212(63), using the values of 70 % deadweight and 75% of the  
509 MCR of the engines and the corresponding reference speed:

$$EEDI = \frac{\left( \prod_{j=1}^M f_j \right) \left( \sum_{i=1}^{n_{ME}} P_{ME(i)} * CF_{ME(i)} * SFC_{ME(i)} \right) + (P_{AE} * CF_{AE} * SFC_{AE})}{f_i * Capacity * V_{ref} * f_w} +$$

510 
$$\frac{\left\{ \left( \prod_{j=1}^M f_j * \sum_{i=1}^{n_{PTI}} P_{PTI(i)} - \sum_{i=1}^{n_{eff}} f_{eff(i)} * P_{AE_{eff}(i)} \right) * CF_{AE} * SFC_{AE} \right\} - \left( \sum_{i=1}^{n_{eff}} f_{eff(i)} * P_{eff(i)} * CF_{ME} * SFC_{ME} \right)}{f_i * Capacity * V_{ref} * f_w} \quad (10)$$

511

512 The minimization of this index is one of the primary targets of the conducted optimization. The  
513 engine power is directly related to the resistance of the hullform, while the deadweight is also  
514 related to both the hullform in terms of displacement and to ship's lightship weight.

515

## 516 2.18 Modeling Uncertainties from Big Data Analysis

517 One of the novel aspects of this methodology has been the use of big data and the statistical  
518 analysis of the latter with the IBM SPSS toolkits for the creation of linear and non-linear  
519 regression formulas as well as probability distribution functions and descriptive statistical  
520 studies. The big data taken into account and analyzed (as already described in the various  
521 subcomponents of the methodology) are in two categories:

522 a. Onboard data (write about their origin) and production of PDF for environmental criteria.

523 The Onboard data were collected from the installed Vessel Performance Monitoring (VPM)  
524 System of a fleet of Capesize and Newcastlemax bulkers that operate both in the Brazil and  
525 Australia trade routes. This VPM system collects real time data (30sec logging and averaging  
526 into 5 minute intervals) of the vessel's Alarm and Monitoring System (AMS) and the vessel's  
527 navigational data from the Voyage Data Recorder (VDR) into an onboard server as per process

528 flow in Figure [4]. This gathering, together with the use of signals from torque meters and flow  
529 meters provides an extensive database that is used for the statistical analysis with the IBM  
530 SPSS toolkit of the following parameters:

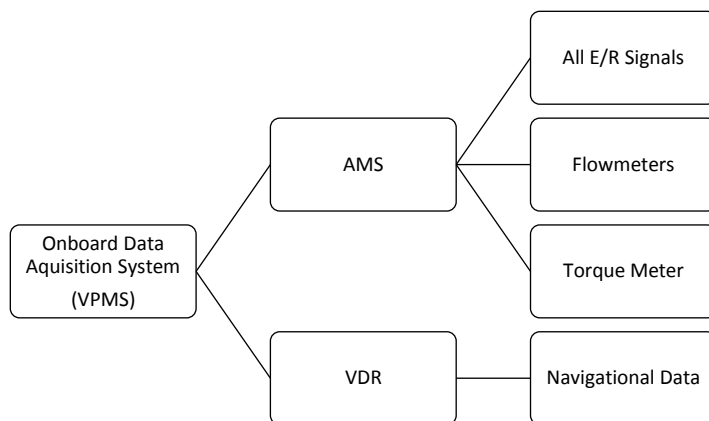
531 1. Operating Speed: Normal PDF with a Mean and Standard Deviation depending on the leg of  
532 the passage.

533 2. Wind Speed: Normal PDF with a Mean and Standard Deviation depending on the leg of  
534 the passage.

535 3. Wind Direction: Normal PDF with a Mean and Standard Deviation depending on the leg of  
536 the passage.

537 4. Current Velocity: Exponential with a scale of around 1 to 1.5 depending on the leg of the  
538 passage.

539 5. Current Direction: Normal PDF with a Mean and Standard Deviation depending on the leg  
540 of the passage.



541

542 Figure 4: Process flow of the data acquisition system

543 b. Clarkson's Ship Intelligence Database for the modelling of market conditions.

544 The Clarkson's Shipping Intelligence Database (Clarkson's [23]) has been used extensively for  
545 the market modeling and studying of the correlations for the following parameters:

546 1. Capesize Earnings (1990 to 2015)

547 Lognormal PDF with Scale=23194.925 and Shape=0.830

548 2. Fuel Price - IFO380 (1990 to 2015)

549 Lognormal PDF with Scale=246.930 and Shape=0.711

550 3. Fuel Price – MGO (1990 to 2015)

551 Triangular PDF with min=101.25, max=1268.13 and mode=120.65.

552

### 553 3 DESIGN CONCEPT

#### 554 3.1 Large Bulk Carrier Market

555 The focus of the present study lies within the large bulk carrier segment. The market for subject  
556 vessel size is positioned on the seaborne transportation of primary bulk commodities for  
557 industrial activities (iron ore, nickel ore and other major minerals) as well as for energy in the  
558 form of coal. As already mentioned, the trade routes for the above mentioned markets are  
559 between Latin America and the Far East (China primarily and then Korea and Japan) as well  
560 as between Australia and again the Far East. The optimal vessel for the maintenance of an  
561 efficient supply chain in these two routes is the primary objective of this study.

#### 562 3.2 Baseline Vessel – 208k Newcastlemax

563 A parent, baseline vessel is herein used as a primary source of reference as well as calibration  
564 for the methodology and all the formulas/computations applied in the latter. The vessel chosen  
565 for this study belongs to the relevant recent segment of Newcastlemax Bulk carriers and is a newly  
566 delivered vessel (2015). The baseline parametric geometry has been adapted to fit the hull form  
567 lines available. As previously mentioned (chapter 2.9.1), the model test results of subject vessel  
568 were used to calibrate and better adapt Holtrop statistical methodology for the prediction of  
569 powering along the entire speed-power curve. The principal particulars of the vessel can be  
570 found in the below table [2]:

571

Baseline Vessel Principal Particulars	
Length over all	299.98
Length between perpendiculars	294
Beam	50
Scantling Draft	18.5
Deck Height	25
Cb	0.8521
Main Engine Specified MCR (kW)	17494 @ 78.7 RPM / MAN B&W 6G70ME-C9.2
Deadweight (tons)	Abt 208,000
Lightship Weight (tons)	26,120
Cargo Hold Capacity (m <sup>3</sup> )	224,712.1

573

Table 2: Baseline Vessel Principal Particulars

## 574 3.3 Proposed Design Concept Characteristics

575 A small Froude number (slow speed) and full hull form is herein proposed as the base hull for  
576 the global optimization. The absence of a bulbous bow is evident as it is a recent trend in bulk  
577 carrier design as such absence assists in the reduction of the vessel frictional resistance (primary  
578 resistance component) while the wave making resistance is not increased. The effect of the  
579 bulbous bow on the above as well as the added resistance are investigated in depth in separate  
580 study. In addition, the use only of an electronically controlled Main Engine is considered and  
581 no Energy Saving Devices (wake equalizing duct, pre-swirl fin, bulbous rudder etc.) are  
582 considered since there is no such device installed on the parent vessel and further to the above  
583 such devices and their effect is to be considered in a post analysis study.

584 3.3.1 Simulation driven design, choice of hullform parameters

585 The assessment of the design is derived from the simulation of the operational, economic and  
586 trading profile (as per methodology in chapter In other words instead of using only one design  
587 point (in terms of draft and speed) multiple points are used derived from actual operating data  
588 of a shipping company.

589 3.4 Optimization Target/Goals

590 The target of any optimization procedure is always to achieve the most desiring  
591 values/properties for the set optimization objectives. The alteration of the designs and assessed  
592 entries is performed through the systematic variation of their distinctive parameters, while each  
593 one of the designs must comply with the set constraints, e.g. stability criteria/maximum  
594 dimensions or deadweight.

595 The generic targets or objectives in almost any ship design optimization problem are:

596 a. Competitiveness

597 The market and economic competitiveness of a an individual vessel variant is the core of any  
598 optimization as a vessel will always be an asset (of high capital value) and can be expressed by  
599 the following indices:

600 1. Required Freight Rate

601 The required freight rate is the hypothetical freight which will ensure a break even for the  
602 hypothetical shipowner between the operating costs, capital costs and its income based on the  
603 annual voyages as well as collective cargo capacity and is such expressed in USD per ton of  
604 cargo.

605 
$$RFR = \frac{OPEX + CAPEX + Fuel\ Costs}{Annual\ Cargo\ Volume}$$

606 2. Operating Expenditure (OPEX)

607 The operating expenditure expressed on a daily cost includes the cost for crewing, insurance,  
608 spares, stores, lubricants, administration etc. It can indicate apart from the operator's ability to

609 work in a cost effective structure, how the vessel's design characteristics can affect. The  
610 lubricant cost is based on actual feed rates used for subject engines as per the relevant service  
611 letter SL2014-537 of MAN [14].

### 612 3. Capital Expenditure (CAPEX)

613 The CAPEX is a clear indication of the cost of capital for investing and acquisition of each  
614 individual design variant. The acquisition cost is calculated from a function derived from actual  
615 market values and the lightship weight for vessels built in Asian shipyards, and more  
616 specifically in China.

### 617 4. Efficiency

618 The merit of efficiency is herein expressed by the IMO EEOI index. Although on the design  
619 basis in practice the IMO Energy Efficiency Design Index is used as a KPI and measure of the  
620 merit of efficiency in new design concepts as well as for any newbuild vessel, in this study the  
621 calculated Energy Efficiency Operating Index is used instead. The reason for this change is the  
622 use of the Operational Profile simulation module based on actual voyage input data for a fleet  
623 of vessels (statistically edited) per each stage of each voyage leg (refer to par. 2.10) thus given  
624 the cargo capacity calculation (par. 2.4) the EEOI can be derived, which can depict more  
625 accurately and realistically the efficiency of the design given the fact that it takes into account  
626 the actual operating profile. The actual transport efficiency of each variant is expressed by a  
627 simple ration of tons of CO<sub>2</sub> emitted to the tons of cargo multiplied by the actual distance  
628 covered. In addition to the above, operational practices such as slow steaming are considered  
629 together with their respective implications (e.g the use of two diesel generators in the normal  
630 sea going condition instead of one in order to cover the blower's electrical load). Furthermore,  
631 the minimization of the required ballast water amount for the ballast conditions is set as  
632 optimization target.

633 3.5 Design Variables

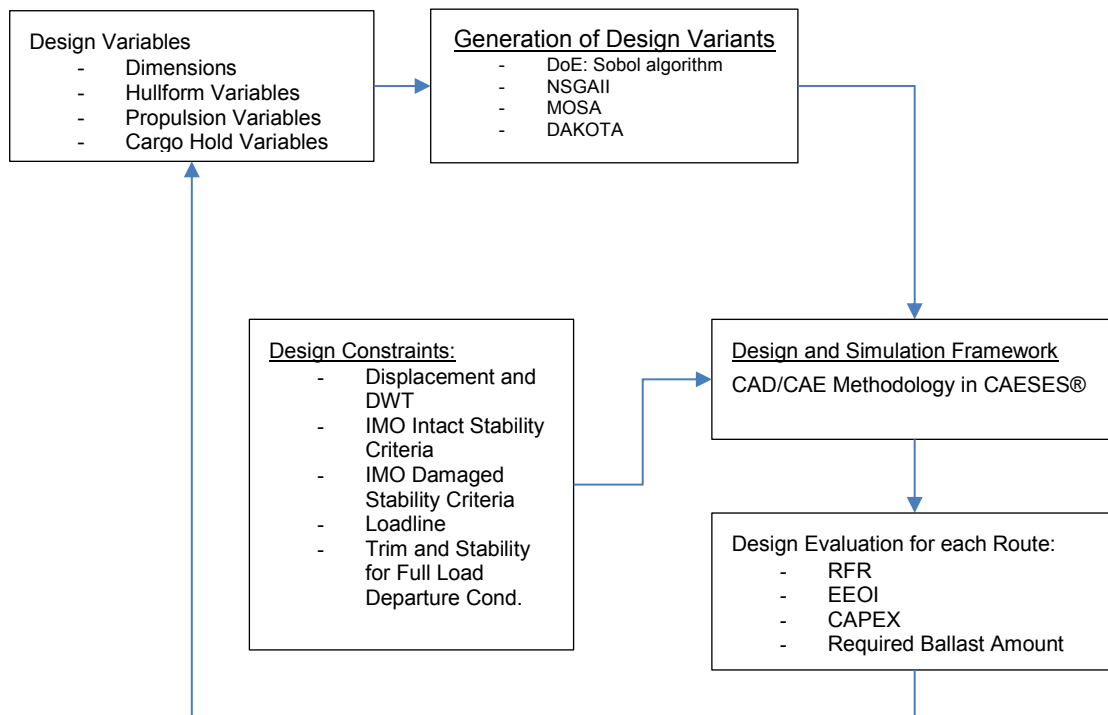
634 From the below table [3], one can identify the selected design variables of the subject  
635 optimization problem. The latter are in three categories; principal dimensions, hull form  
636 characteristics (Cb, LCB and Parallel Midbody) and cargo hold arrangement parameters. The  
637 more detailed design variables of the hull form arrangement for the detailed shape of the  
638 bulbous bow (if any), flair and stem shape as well as stern shape are going to be assessed in a  
639 separate optimization study with the use of integrated CFD codes.

<b>Design Variable</b>	<b>Lower Boundary</b>	<b>Upper Boundary</b>
Length between Perpendiculars	275	320
Length Overall	280	325
Beam	42	55
Draft	16.5	19.5
Deck height	24	27
Hopper Height	7	10
Hopper Breadth (m)	2.5	4
Topside Height (m)	5	9
Topside Breadth (m)	8	12
Inner Bottom Height (m)	2	3
Block Coefficient Cb	0.84	0.87
LCB (%Lbp)	0.49	0.55
Bilge Height (m)	2.4	8
Bilge Width (m)	2.4	8
Propeller Diameter (m)	8	10
Propeller Expanded Area Ratio	0.35	0.55
Propeller Pitch over Diameter	0.75	1.2

640 Table 3: List and range of design variables of the optimization problem.

641 3.6 Optimization Procedure

642 The optimization procedure applied for this study follows the rational of any optimization loop  
643 in engineering as it is evident from Figure [5].



644

645

Figure 5: The optimization Loop applied.

646

For each iteration of the same loop the design variables receive their input values from the

647

«design engine» applied in the CAESES. The design engine can either be a random number

648

generator or an optimization algorithm depending on the optimization stage. The applied values

649

then trigger the generation of a new variant from the holistic, parametric model that utilizes the

650

developed methodology for that matter.

651

After the variant generation, the Design Objectives, which are selected as the measures of merit

652

of each variant are logged and assessed accordingly while at the meantime the Design

653

Constraints imposed are checked for compliance. The Design constraints chosen for this

654

application were the calculated values for Deadweight, Cargo Specific Gravity and the Stability

655

Criteria of the 2008 Intact Stability Code. The size restrictions (in terms of vessel's dimensions)

656

were not used in constraints given the fact they were taken into account in the applied range of

657

the Design Variables.

658 The optimization procedure described in this paper can be described as a stepped (multi stage)  
659 one. At first, it is necessary to explore and fully understand both the design space (potential for  
660 improvement with given constraints) as well as the sensitivity of the methodology by a Design  
661 of Experiments procedure, using a system available random number generator that follows the  
662 Sobol sequence procedure [30]. The sensitivity analysis is a very important, preparatory step  
663 in which it is ensured that no major, unreasonable manipulations occur. In addition to that it is  
664 important to see that the results are realistic both on a quantitative and qualitative basis, with  
665 the latter in need of particular attention since the design ranking and selection is the essence of  
666 optimization (the value of a favored design is not important than the relationship with all the  
667 other produced designs).

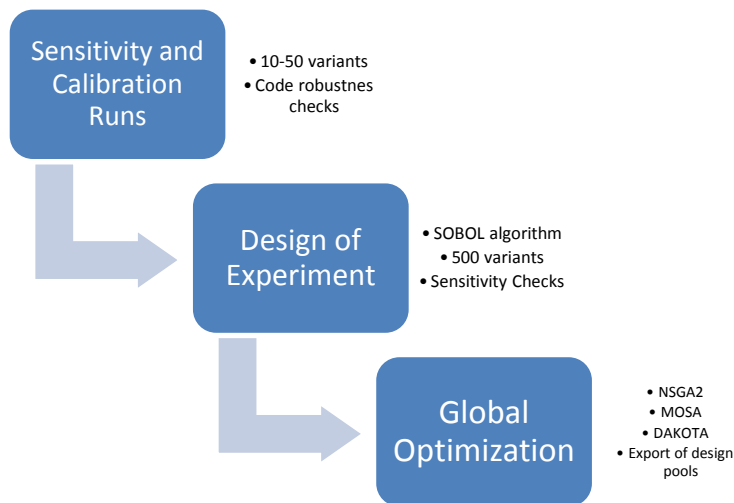
668 The following formal optimization runs utilize genetic algorithm techniques (NSGA II  
669 algorithm [28]). The formal optimization runs involve the determination of the number of  
670 generations and the definition of population of each generation to be explored. Then the  
671 generated designs are ranked according to a number of scenarios regarding the mentality of the  
672 decision maker. One favored design is picked to be the baseline design of the next optimization  
673 run, where the same procedure is followed. When it is evident that there little more potential  
674 for improvement the best designs are picked using the same ranking principles with utility  
675 functions, and are exported for analysis.

676 Both the SOBOL and NSGA II algorithms as well as a plethora of other variant generation and  
677 optimization algorithms are fully integrated and available within the CAESES.

678

679

680



681

682

Figure 6: The different Optimization Stages.

### 683 3.7 Design of Experiment (DoE)

684 The Design of Experiment has the primary purpose of the calibration, test and sensitivity check  
 685 of the methodology DoE serving as an exploitation step. The computational power required is  
 686 small and a fast first impression of the design space is given. From the first indications, as  
 687 anticipated, there is a strong scale effect which one can say that dominates this particular  
 688 optimization problem. This effect is very common in ship design where the largest vessels  
 689 usually dominate the smaller since the increase of cargo capacity does not trigger an equivalent  
 690 increase in the powering requirements or the vessel's weight. In addition to the scaling effect  
 691 it was observed as in the formal optimization algorithm that there was a strong linear correlation  
 692 between the Required Freight Rate (RFR) and the EEOI, which was also anticipated since both  
 693 functions use cargo capacity. The feasibility index was in a very high level (above 90%). In  
 694 total 250 designs were created.

### 695 3.8 Global Optimization Studies

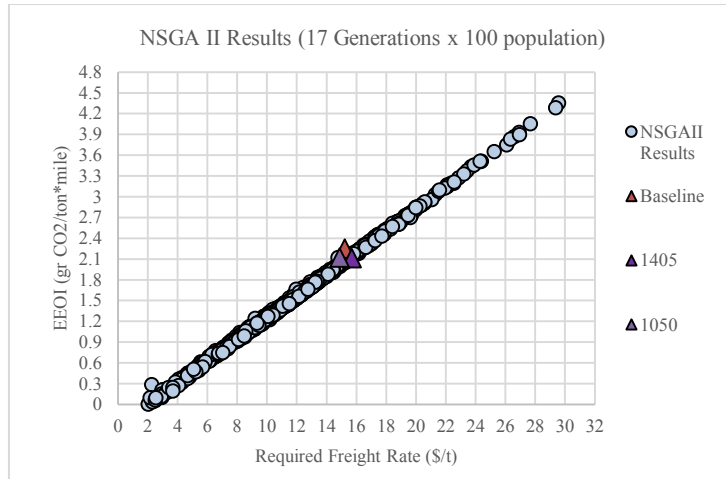
696 In this stage of the formal, global design optimization the NSGA II algorithm is utilized. The  
 697 latter is a genetic, evolutionary algorithm that is based on the principles of biological evolution  
 698 (Darwin [10]). As in the biological evolution each design variant is an individual member of a  
 699 population of a generation. Each individual of the population is assessed in terms of the

700 Optimization Objectives, as well as its relation to the desired merits. For the application in ship  
701 design optimization it is usual to apply a large population for each generation with an adequate  
702 number of generations. The large population combined with a high mutation probability  
703 ensures that the design space is properly covered, while the number of generations ensures that  
704 there is a push towards the Pareto frontier for each case of objective combination. For this  
705 particular application a combination of 17 generations with 100 variants population each was  
706 selected. The mutation probability was increased from the default value by CAESES of 0.01  
707 to 0.05 in order to increase mutation events that trigger the variation of the design variables  
708 and thus have a wider design space.

709 In Figure [6], the scatter plot of the generated design population is depicted, with the RFR of  
710 each design on the x-axis and the respective EEOI on y-axis. A distinctive linear correlation  
711 between the EEOI and RFR is evident. This has been observed regardless of the use of  
712 uncertainty functions and is attributed to the direct linear correlation of the fuel consumed and  
713 CO<sub>2</sub> emissions (through the carbon conversion factors). We can see that the both the baseline  
714 as well as dominant variants are close to the middle of the straight cloud line comprised by the  
715 generated designs. It should be noted that the vessels with lower RFR has significantly  
716 increased OPEX and Required Ballast Water amount values making them thus less favored in  
717 the decision making process.

718 In Figure [7], the scatter plot of the RFR vs CAPEX is found. A clear Pareto frontier is  
719 formulated on which the decrease of CAPEX triggers in turn an increase in the RFR. This  
720 pattern can be attributed to the fact that these two objectives are contradicting. The RFR can  
721 be decreased by the increase of cargo carrying capacity (and thus income) but this in turn will  
722 increase the vessel size and thus building cost. The CAPEX comprises the acquisition (new  
723 building) cost and dry-docking costs both of which have been formulated as a non-linear  
724 function of the vessel's lightship. Rather interestingly, the baseline design is far from the pareto

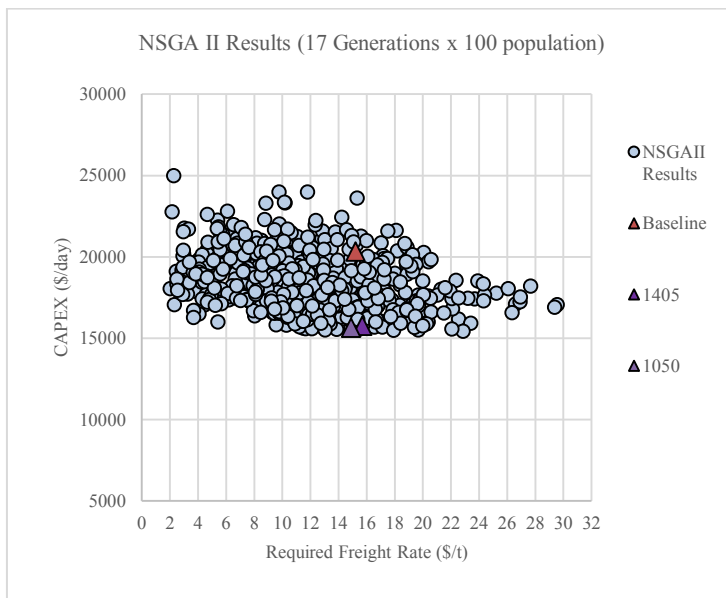
725 frontier to an increased CAPEX compared to the dominant variants, which have the smallest  
726 CAPEX values. The scatter plot of the RFR vs the OPEX (Figure [8]), shows the same pattern  
727 as the previous plot of CAPEX. Again here, the relationship of RFR to OPEX is antagonistic  
728 as the larger vessels with lower RFR values will have larger installed engines which will have  
729 significantly higher maintenance costs (non-linear function of vessel's SMCR) and require  
730 higher crewing and insurance costs (non-linear function of the vessel's GT). Like in the case  
731 of CAPEX the baseline design has a distance from the frontier, but in this case this is smaller  
732 due to the small OPEX of this vessel. Lastly, an interesting and clear Pareto frontier is observed  
733 in the scatter plot between the Required Ballast Water Amount and the vessel's OPEX. Here,  
734 the increase of Required Ballast will also correspond to an increase of the OPEX, which is  
735 rather sharp. The front is therefore localized at the bottom left corner of the graph. The  
736 underlying mechanism between this relationship is that the Ballast Water amount required,  
737 determines the ballast pumps capacity and in turn the Ballast Water Treatment System (BWTS)  
738 capacity and both of them Auxiliary Engines rating. The running cost of the BWTS is a  
739 significant component of the OPEX, both due to the higher maintenance costs of the electric  
740 generating plant but due to the cost of chemicals both for treatment and neutralization. The  
741 same will also apply for the relationship of Required Ballast Amount with CAPEX since the  
742 cost of the installation of the BWTS system is significant and an exponential function of the  
743 Ballast Pumps Capacity which is calculated basis on the Required ballast amount and ballasting  
744 and de-ballasting time (constant).



745

746

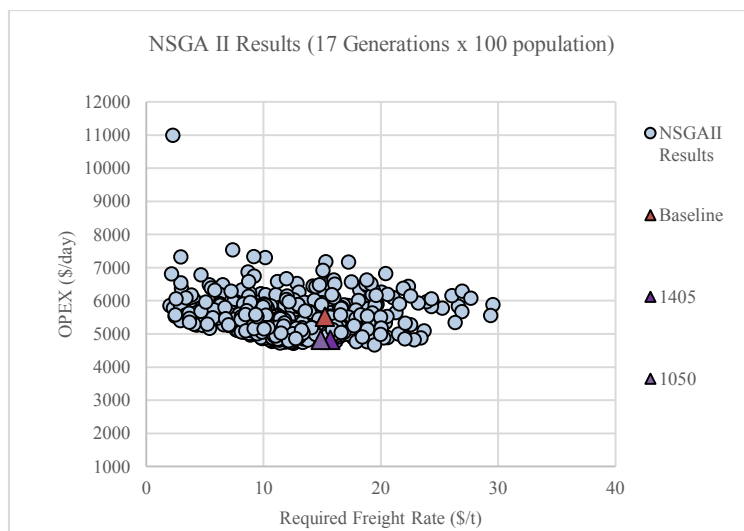
Figure 7: Scatter plot of the Optimization Results: RFR vs EEOI



747

748

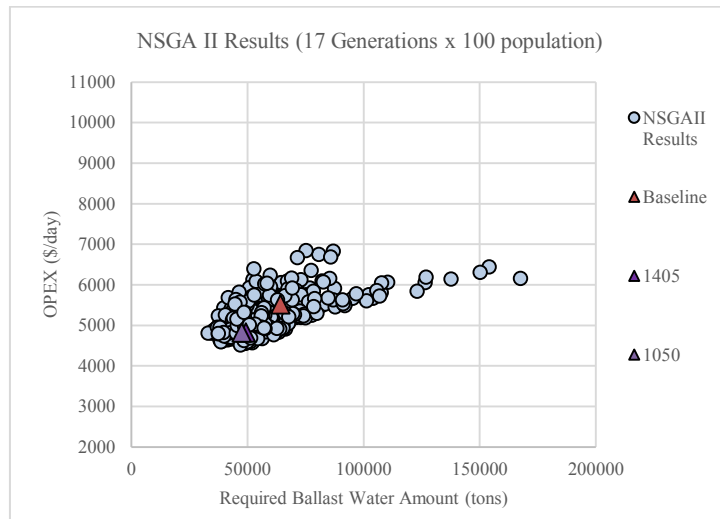
Figure 8: Scatter plot of the Optimization Results: RFR vs CAPEX



749

750

Figure 9: Scatter plot of the Optimization Results: RFR vs OPEX



751

752 Figure 10: Scatter plot of the Optimization Results: Required Ballast Water Amount vs

753

OPEX

### 754 3.9 Dominant Variant Ranking

755 One of the most critical steps during optimization of any system is the selection and the sorting  
 756 of the dominant variants. For this particular reason it is necessary to follow a rational, rather  
 757 than an intuitive, approach in order to consider in an unbiased way all trade-offs that exist. One  
 758 such method is utility functions technique.

759 The optimum solution in our case would dispose the minimum EEOI, RFR, OPEX and CAPEX  
 760 values. Instead of using fixed weights for the set criteria in the evaluation of the variants, we  
 761 rather assume a utility function as following

$$762 \quad U = w_{EEOI} * u(EEOI) + w_{RFR} * u(RFR) + w_{CAPEX} * u(CAPEX) + w_{OPEX} * u(OPEX) \quad (11)$$

763 The utility of each design variant with regards to the optimization targets is normalized by the  
 764 best attained KPI valuation of each design population. The weights assigned for each respective  
 765 KPI of each variant are a linear function of the distance of the attained utility value to the  
 766 maximum utility value (under the normalization has a value of 1) of the design population. The  
 767 design population is in turned ranked in a descending order from the maximum to minimum  
 768 attained utility as per equation (20). The top 10 most favourable designs are selected for each

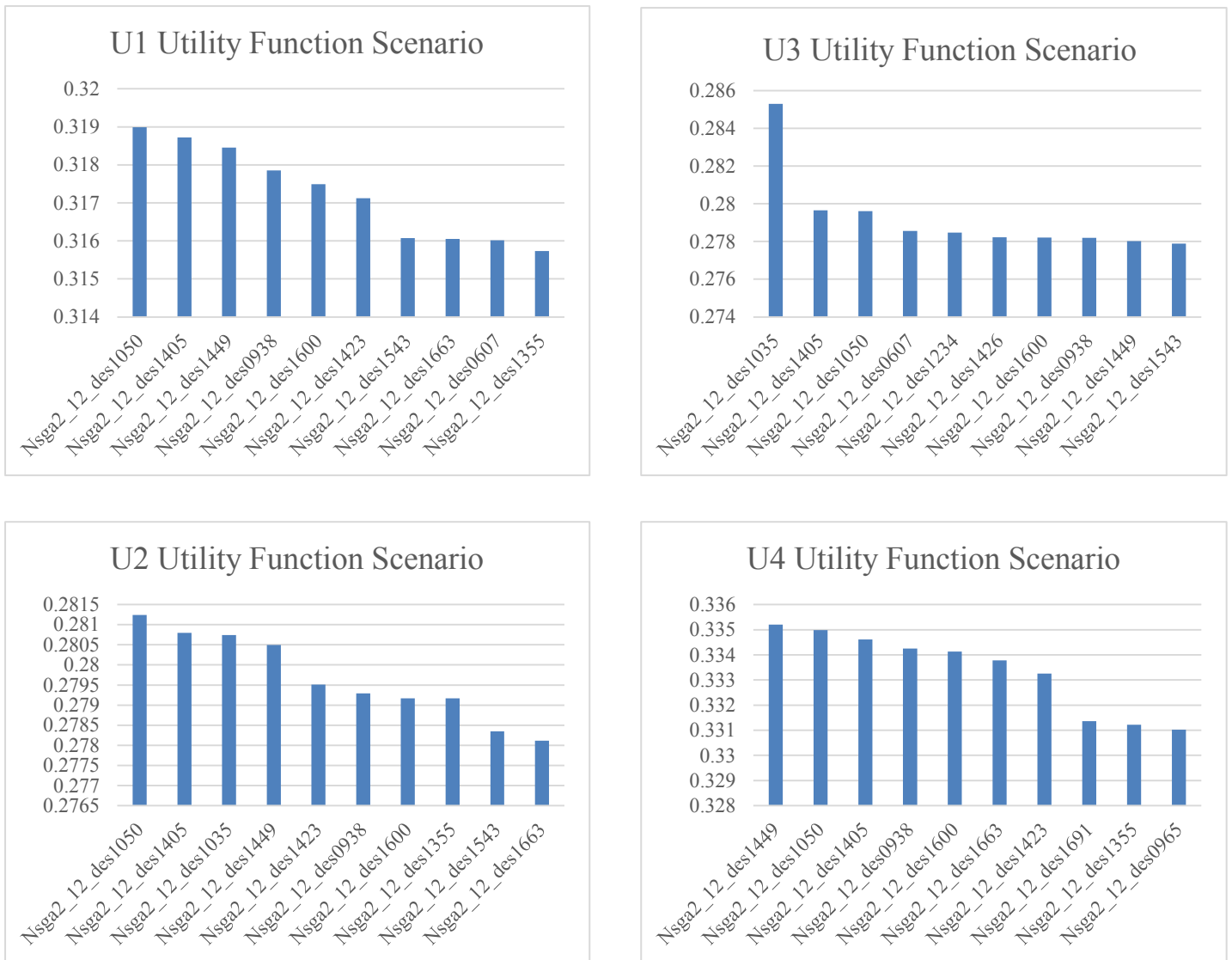
769 maximum weight scenario (Table [4]) as dominant variants resulting in the identification and  
770 sorting of 40 designs with best performance according to each utility scenario.

Maximum Objective Weight	U1	U2	U3	U4
RFR	0.2	0.3	0.2	0.1
EEOI	0.2	0.1	0.1	0.3
OPEX	0.2	0.1	0.3	0.1
CAPEX	0.2	0.2	0.1	0.3
Required Ballast Water Amount	0.2	0.3	0.3	0.2

771

Table 4: Weights used for the utility functions

Figure 11: Ranking of Dominant Variants with U1-U4 Scenario



Particulars	Baseline	ID1405	ID1050	ID1035
Lbp (m)	294	275	276.1	277.8
Beam (m)	50	42.15	42.353	42.718
Deck Height (m)	25	25	25.26	26.53
Cb	0.8538	0.8599	0.8555	0.844
LCB	0.51986054	0.52	0.499	0.5480
LOA (m)	299.98	279	278	278.7
Draft (m)	18.5	16.59	17.02	16.93

Topside Breadth (m)	12	8.27	11.33	9.468
Topside Height (m)	9	5.15	7.71	5.024
Hopper Height (m)	10	9.98	9.046	8.529
Hopper Breadth (m)	4	3.25	3.42	3.412
Double Bottom Height (m)	2.5	2	2.85	2.14
Propeller Diameter (m)	9	9.27	8.87	8.05
Propeller P/D	0.9	0.942731	0.763	0.804
Propeller Expanded Area Ratio	0.55	0.516	0.4544	0.459
Bilge Height (m)	2.4	5.19	2.16	6.901
Bilge Width (m)	2.4	6.06	2.58	2.512

774 Table 5: Principal Particulars of baseline and dominant variants

775 From the above ranking (Figures [10 to [13]) it is very interesting to observe that there is a  
776 certain repetition in the top three dominant variants from the ranking procedure. Furthermore,  
777 for scenario U3 where there is an equal weight for all objectives, the three top dominant variants  
778 are the ones from scenario's U1 and U2. All the above illustrate that the peak on the observed  
779 pareto front is strong and apart from that, the dominant variants that can be selected (e.g. #1405,  
780 #1050, #1035) perform better in a robust way under different assumptions and weights from  
781 the decision maker point of view. The characteristics of these three variants can be found in  
782 the table [5].

783

#### 784 4 DISCUSSION OF THE RESULTS- FUTURE RESEARCH

785 From the table [6] below, we can observe that for design #1405 an increase of the RFR of 3%  
786 was observed with a decrease however of the EEOI by 6%, of the OPEX by 12% and CAPEX  
787 and Required Ballast Water amount by 23%. Design #1050 seems to be more promising as the  
788 improvements in EEOI, OPEX, CAPEX and Required Ballast Amount are marginally higher

789 than these of the #1405, however the RFR is 2.23% lower than that of the baseline. The  
 790 marginal reduction of the RFR can be justified by the reduction of generally vessel size  
 791 primarily in terms of beam and length (beam given the fact that these vessels are not stability  
 792 limited) and thus the reduction of the initial capital cost, while in the meantime the cargo  
 793 capacity has inevitably decreased, reducing thus the profitability of the vessel.

Particulars	Baseline	1405	Difference %	1050	Difference %
RFR	15.22	15.69	3.09	14.88	-2.23
EEOI	2.25	2.11	-6.22	2.12	-5.78
OPEX	5520	4827	-12.55	4823	-12.63
CAPEX	20322	15771	-22.39	15648	-23.0
Required Ballast Water Amount	64244	49298	-23.26	47616	-25.88

794 Table 6: Design Objectives of the Baseline vs the Dominant Variants

795 From the above discussion we can conclude that the novel methodology herein proposed for  
 796 the simulation driven design with lifecycle, supply chain and the actual operating in service  
 797 parameters can successfully trigger a reduction in the RFR and EEOI via systematic variation  
 798 and advanced optimization techniques. However, this is a preliminary work restricted only into  
 799 illustrating the applicability and potential of this method.

800

## 801 ACKNOWLEDGEMENTS

802 The authors would like to express their deep gratitude to their mentor and teacher, Professor  
 803 Apostolos Papanikolaou, Ship Design Laboratory, National Technical University of Athens,  
 804 whose lectures on ship design and holistic optimization have been the inspiration for this paper.  
 805 Furthermore, authors would like to acknowledge the help of Star Bulk Carriers Corporation in  
 806 providing valuable data from their operating fleet and reference drawings. Dr. Boulougouris

807 work was supported from DNVGL and RCCL, sponsors of the MSRC. The opinions expressed  
808 herein are those of the authors and do not reflect the views of DNVGL and RCCL.

809

## 810 REFERENCES

- 811 [1] Stopford M. , “Maritime Economics 3<sup>rd</sup> Edition”, Routledge, ISBN 978-0-415-27558-3
- 812 [2] United Nations Conference on Trade and Development, “Review of Maritime Transport  
813 2017”, UNCTAD secretariat calculations, based on data from Clarksons Research, 2017.
- 814 [3] Papanikolaou A., Holistic ship design optimization. Computer-Aided Design,  
815 doi:10.1016/j.cad.2009.07.002, 2009
- 816 [4] IMO, 2008 Intact Stability Code, Res. MSC.267(85), December 2008.
- 817 [5] Holtrop J., Mennen G.G.J., An approximate power prediction method, International  
818 Shipbuilding Progress 1982
- 819 [6] Papanikolaou A., “Ship Design - Volume A: Preliminary Design Methodology”, Publ.  
820 SYMEON, 1988/1989, 2nd edition: 1999 (Greece).
- 821 [7] MAN B&W, Marine Engine Program 2015
- 822 [8] Nikolopoulos L. "A Holistic Methodology for the Optimization of Tanker Design and  
823 Operation and its applications", Diploma Thesis NTUA, July 2012.
- 824 [9] Darwin C., "On the origin of species by means of natural selection, or the preservation of  
825 favored races in the struggle for life", London: John Murray. [1st ed.], 1859.
- 826 [10] Abt C., Harries S., "Hull Variation and Improvement using the Generalised Lackenby  
827 Method of the FRIENDSHIP-Framework", The Naval Architect, RINA © September 2007.
- 828 [11] Koutroukis G., "Parametric Design and Multi-objective Optimization-Study of an  
829 Ellipsoidal Containership", Diploma Thesis NTUA, January 2012.
- 830 [12] Kwon, Y.J. (2008). “Speed Loss Due To Added Resistance in Wind and Waves”, the  
831 Naval Architect, Vol. 3, pp.14-16

- 832 [13] Lu R., Turan O., Boulougouris E., Banks C., Incecik A., “A semi-empirical ship  
833 operational performance prediction model for voyage optimization towards energy efficient  
834 shipping”, *Ocean Engineering*, 110, p 18-28, 2015.
- 835 [14] MAN Diesel and Turbo, Service Letter SL2014-587 «Guidelines of Cylinder  
836 Lubrication», Copenhagen 2014.
- 837 [15] Nikolopoulos L., Boulougouris E., ‘Applications of Holistic Ship Theory in the  
838 Optimization of Bulk Carrier Design and Operation’, EUROGEN 2015 Conference, September  
839 2015 Glasgow.
- 840 [16] Nikolopoulos L., Boulougouris E., “A Study on the Statistical Calibration of the Holtrop  
841 and Mennen Approximate Power Prediction Method for Full Hull Form Vessels, Low Froude  
842 Number Vessels”, *SNAME Journal of Ship Production and Design*, Vol., Month January 2018,  
843 pp 1-28.
- 844 [17] Bernitsas M.M., Ray D., Kiley P., “ $K_T$ ,  $K_Q$  and Efficiency Curves for the Wageningen B-  
845 Series Propellers”, University of Michigan, Report No.237, May 1981.
- 846 [18] [MEPC 68] – Publication of ISO15016:2015, Ships and marine technology – Guidelines  
847 for the assessment of speed and power performance by analysis of speed trial data, IMO,  
848 February 2015.
- 849 [19] International Marine Coatings, Propeller No.15, January 2003.
- 850 [20] International Marine Coatings, Propeller No.16, August 2003.
- 851 [21] Clarksons Shipping Intelligence database (<https://sin.clarksons.net/>)
- 852 [22] Fujiwara, T., Ueno, M. and Ikeda, Y. (2005), “A New Estimation Method of Wind Forces  
853 and Moments acting on Ships on the basis of Physical Component Models”, *J. of The Japan*  
854 *Society of Naval Architects and Ocean Engineers*, 2, 243-255.
- 855 [23] Liu S., Shang B., Papanikolaou A., Bolbot V., “An Improved Formula for Estimating the  
856 Added Resistance of Ships in Engineering Applications”, *J. Marine. Sci. Appl.* (2016) 15: 442.

- 857 [24] Marine Environment Protection Committee (MEPC), 66th session, 31 March to 4 April  
858 2014.
- 859 [25] Cichowicz J., Theotokatos G., Vassalos D., (2015), “Dynamic Energy Modelling for ship  
860 life-cycle performance assessment”, *Journal of Ocean Engineering* 110 (2015).
- 861 [26] Deb K., Pratap A., Agarwaj S., Meyarivan T. (2002), “A fast and elitist multiobjective  
862 genetic algorithm: NSGA-II”, *IEEE Transaction on Evolutionary Computation*, Volume 6,  
863 Issue 2, April 2002.
- 864 [27] Ulungu E.L, Teghem J., Fortemps P.H, Tuyttends D. (1999), “MOSA method: a tool for  
865 solving multiobjective combinatorial optimization problems” *Journal of Multi-Criteria*  
866 *Decision Analysis*, Volume 8, Issue 4, July 1999.
- 867 [28] Sobol, I. M. (1976) "Uniformly distributed sequences with an additional uniform  
868 property". *Zh. Vych. Mat. Mat. Fiz.* 16: 1332–1337 (in Russian); *U.S.S.R. Comput. Maths.*  
869 *Math. Phys.*16: 236–242 (in English).
- 870 [29] LACKENBY, H (1950), “On the Systematic Geometrical Variation of Ship Forms”,  
871 *Trans. INA*, Vol. 92, pp. 289-315.
- 872 [30] Alwan, S., n.d. Simulation-based ship design and system engineering, RINA, Energy  
873 Efficient Ships 2016, November 2016, pp.9.
- 874 [31] Aristotle & Ross, W. D., 1981. *Aristotle's Metaphysics*. Oxford [England], Clarendon  
875 Press.
- 876 [32] Diez, M. & Peri, D., 2010. Two-stage Stochastic Programming Framework for Ship  
877 Design Optimization under Uncertainty. s.l., s.n.
- 878 [33] Diez, M., Peri, D., Fasan, G. & Campana, E., 2010. Multi-Disciplinary Robust  
879 Optimization for Ship Design. Pasadena, California, s.n.
- 880 [34] Good, N., 2006. Multi-Objective Design Optimization considering Uncertainty in a Multi-  
881 Disciplinary Ship Synthesis Model. Master Thesis, Virginia Tech, Blacksburg , Virginia.

882 [35] Hannapel, S., 2012. Development of Multidisciplinary Design Optimization Algorithms  
883 for Ship Design under Uncertainty. PhD Thesis, University of Michigan.

884 [36] Hannapel, S. & Vlahopoulos, N., 2010. Robust and Reliable Multidiscipline Ship Design.  
885 AIAA/SSMO Multidisciplinary Analysis Optimization Conference, Fort Worth, Texas,  
886 American Institute of Aeronautics and Astronautics.

887 [37] Koutroukis, G. et al., 2013. Multi-Objective optimization of a containership design.  
888 Mediterranean Marine Science.

889 [38] Nikolopoulos, L. et al., 2014. Holistic Approaches in Containership Design. London, UK,  
890 Royal Institution of Naval Architects.

891 [39] Papanikolaou, A., 2010. Holistic ship design optimization. Computer-Aided Design, Issue  
892 42, pp. 1028-1044.

893 [40] Papanikolaou, A., Harries, S., Wilken, M. & Zaraphonitis, G., 2011. Integrated Ship  
894 Design and Multiobjective Optimization Approach to Ship Design, 15<sup>th</sup> Int. Conference on  
895 Computer Application in Shipbuilding, ICCAS, Trieste, Italy.

896 [41] Papanikolaou, A., Tuzcu, C., Tsihchlis, P. & Eliopoulou, E., 2007. Risk-Based  
897 Optimization of Tanker Design. 3<sup>rd</sup> Int. Maritime Conference on Design for Safety, September  
898 2007.

899 [42] Papanikolaou, A. et al., 2010. Optimization of an AFRAMAX Oil Tanker Design. Journal  
900 of Marine Science and Technology, 15(4).

901 [43] Priftis, A., Turan, O. & Boulougouris, E., 2018. Parametric design and holistic  
902 optimization of post-panamax containerships. International Marine Design Conference  
903 (IMDC) 2018, Helsinki, Finland, Taylor and Francis Group.

904 [44] Sames, P. et al., 2011. BEST Plus – Better Economics with Safer Tankers. Houston Texas,  
905 Society of Naval Architects and Marine Engineers (SNAME).

906 [45] Sandvik, E., Asbjornlett, B., Steen, S. & Johnsen, T., 2018. Estimation of fuel  
907 consumption using discrete-event simulation – a validation study. International Marine Design  
908 Conference (IMDC) 2018, Helsinki, Finland, Taylor and Francis Group.

909 [46] Smuts, H. J., 1927. Holism and Evolution. 1st ed. London: Macmillan and Company  
910 Limited.

911 [47] Sountanias, I., 2014. Parametric Ship Design and Holistic Design Optimization of a 9000  
912 TEU Container Carrier. Athens, Greece: National Technical University of Athens.

913 [48] Tillig, F., Ringsberg, J., Mao, W. & Ramme, B., A generic energy systems model for  
914 efficient ship design and operation, Proceedings of the Institution of Mechanical Engineers,  
915 Part M: Journal of Engineering for the Maritime Environment, Vol 231, Issue 2, 2017, pg. 649–  
916 667.

917 [49] Little, Roderick J A, and Donald B Rubin. 2019. Statistical Analysis with Missing Data.  
918 3rd ed. Vol. 793. John Wiley & Sons.

919 [50] Nguyen, Cattram D., John B. Carlin, and Katherine J. Lee. 2017. “Model Checking in  
920 Multiple Imputation: An Overview and Case Study.” Emerging Themes in Epidemiology 14  
921 (1): 1–12. <https://doi.org/10.1186/s12982-017-0062-6>.

922